Bachelor's thesis

Numerical analysis of the effects of an applied magnetic field on the vortex-assisted photon count of SNSPDs

Georg J. Meili

Supervisor: Dr. A. Engel
Group: Prof. Dr. A. Schilling

Table of contents

1) Introduction

Superconducting nanowire single-photon detectors (SNSPDs) are very effective detectors compared to other detector types, in terms of speed, low dark count rate and photon energy range. These structures can be used to detect photons with much lower energies compared to the semiconductor detectors, since the bandgap there tends to be of the order of 1 eV. A silicon single-photon detector cannot detect photons with wavelengths greater than 1000 nm for example, because it has a bandgap of 1.5 eV. In most semiconductor single-photon detectors, Fermi-excitations are necessary in order to detect a photon. In superconductors, with the same photon energies, many more excitations are created.

Potential applications of this technology are in the area of optical quantum information, like the quantum key distribution [12], where a wider spectral range is needed, with smaller dead time, small dark count rate, a great detection efficiency and low timing jitter (variation in the time interval between the absorption of a photon and the generation of an output electrical pulse from the detector), and the ability to resolve the photon number, which is difficult with SNSPDs [12] since most of them can only distinguish between zero or 'one or more' photon absorptions.

If an absorbed photon has enough energy to make the whole cross-section of the SNSPD normal conducting, we will have a detection event. In general, it has to be assumed that visible and near-infrared photons with energies of about 1 eV do not have sufficient energy. In this case, there are many mechanism that have been discussed over the years that can lead to a detection event. One possible mechanism, and the one that will be discussed in this thesis, is that a photon absorbed anywhere in the strip can reduce the edge barrier so much that a vortex will enter without additional thermal activation energy, and this will lead to a photon count.

For these vortex-assisted photon counts, the photon count rate rises for increasing applied current and has a plateau at higher currents near the critical current. It will be assumed that a magnetic field perpendicular to the strip plane does not affect the formation of hot spots by photons, but still increases the photon count rate.

The goal of this work is to define the minimal applied magnetic field necessary, given a bias current, in order to have 100% probability of vortex crossing in the case of one photon absorption of a given energy. That is, to be 100% sure that each single photon will be detected for the vortex-assisted photon counts.

The detection process is actually not clear and under active investigation. Different models have been proposed and the magnetic field dependence may help to differentiate between models.

2) Physical Background

2.1. Basic Phenomena

Superconductivity is the name for the phenomenon of zero electrical resistance (R = 0 Ω) and perfect diamagnetism (χ = -1) that occurs in certain materials when cooled below a critical temperature $\mathrm{T_c}$ that is material dependent.
It is characterized by the Meissner effect, a complete expulsion of magnetic field lines from the inside of the superconductor. Not only that a magnetic field cannot enter the superconductor, but also a field in an originally normal sample is expelled as it is cooled below $\mathrm{T_c}$.

The superconducting state is defined by three very important factors: critical temperature (T_c), critical field (H_c), and critical current density (j_c). Each of these parameters is dependent on the other two properties present. Maintaining the superconducting state requires that the magnetic field, the current density, as well as the temperature, remain below the critical values, all of which depend on the material. An illustration of a critical surface formed by these three parameters can be seen in figure 1. When electrons form Cooper pairs, they can share the same quantum wave-function or energy state. This results in a lower energy state for the superconductor. T_c and H_c are values where it becomes favorable for the electron pairs to break apart. The current density larger than the critical value is forced to flow through normal material.

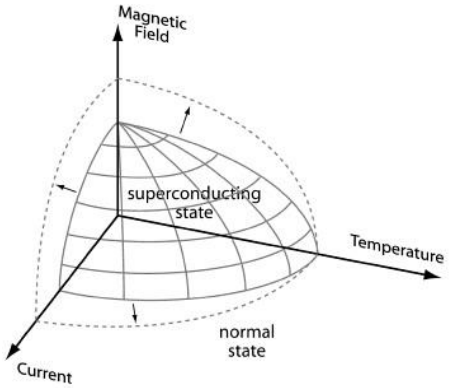

FIGURE 1: [9] Sketch of the critical surface that separates the superconducting from the normal state in the parameter space span by temperature, magnetic field and current.

2.2. Discovery

Superconductivity was discovered in 1911 by Heike Kamerlingh Onnes. Three years earlier he liquefied helium for the first time, and this gave him the refrigeration technique required to reach very low temperatures of a few Kelvin. He was studying the resistance of solid mercury at these temperatures, and observed that at a temperature of $\sim 4.2\ \mathrm{K}$, the resistance abruptly disappeared. His original experimental measurements can be seen in figure 2.

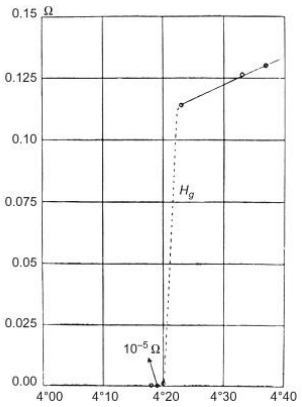

FIGURE 2: The discovery of superconductivity by Kamerlingh Onnes [8]

2.3. Meissner effect

When a weak external magnetic field *H* is applied, and the superconductor is cooled down below its critical temperature, the magnetic field is expelled. The Meissner effect does not completely force out the field, but instead it penetrates the superconductor to a very small distance, called the London penetration depth λ, decaying exponentially to 0 within the material. The typical penetration depth is on the order of 100 nm.
A phenomenological explanation was given by Fritz and Heinz London, who, modifying the essential equations of electrodynamics, predicted that the magnetic field H in a superconductor decays exponentially from whatever value it possesses at the surface, with penetration depth λ.

$$\nabla^2 \mathrm{H} = \frac{\mathrm{H}}{\lambda^2} \tag{1}$$

with

$$\lambda^2 = \frac{\varepsilon_0 \mathrm{m} c^2}{\mathrm{n_s} e^2} = \frac{\mathrm{m}}{\mu_0 \mathrm{n_s} e^2} \ , \tag{2}$$

where m is the mass of the superconducting carrier and n_s the superconductor carrier density.

The most important consequence is that electromagnetic fields are screened from the interior of a bulk superconductor in a characteristic penetration depth λ given by (2). This is the characteristic length of the fall-off of a magnetic field due to surface currents. For example, a magnetic field H parallel to the surface would decrease exponentially into the interior of a bulk superconductor as

$$\mathrm{H(x)} = \mathrm{H(0)} e^{-\frac{\mathrm{x}}{\lambda}} \ , \tag{3}$$

where x is measured from the surface.

For the case of a flat superconducting slab of finite thickness d in an applied magnetic field H_a , solving (1) with the boundary conditions that $H = H_a$ at the 2 surfaces $x = \mp \frac{d}{2}$, one obtains a superposition of exponentials penetrating from both sides, so that

$$H = H_a \frac{\cosh(\frac{x}{\lambda})}{\cosh(\frac{\mathrm{d}}{2\lambda})} \tag{4}$$

that is, H is reduced to a minimum value at the middle of the strip.

2.4. Ginzburg-Landau theory

In some cases, the Meissner effect is not absolute. In type II superconductors, magnetic flux can penetrate into the bulk of the material, but does so in discrete units of $\phi_0 = \mathrm{h}/2\mathrm{e}$, the magnetic flux quantum. In type I superconductors, there is some critical field above which the entire sample goes normal-conducting.
There is no way to explain this using classical mechanics. So, a superconducting order parameter $\Psi(\boldsymbol{r})$ was introduced by Ginzburg and Landau in 1950 to describe the superconducting properties, related to the density of superconducting electrons with $|\Psi(\boldsymbol{r})|^2 \propto n_s(\boldsymbol{r})$, where $\Psi(\boldsymbol{r}) = 0$ if $T > T_c$ (the material is not superconducting) and $\Psi(\boldsymbol{r}) \neq 0$ if $T < T_c$ (superconducting state).
In this theory, all characteristics and properties of superconductivity follow from the Ginzburg-Landau free energy [2]:

$$f = f_n + \alpha|\Psi|^2 + \frac{\beta}{2}|\Psi|^4 + \frac{1}{2m}|(-i\hbar\nabla - 2\mathrm{e}\mathbf{A})\Psi|^2 + \frac{\mu_0|H|^2}{2}, \tag{5}$$

where f_n is the free energy in the normal state, α and β temperature dependent phenomenological parameters, m is the effective mass, e the electron charge, **A** the electromagnetic vector potential and H an applied magnetic field.
By minimizing the free energy with respect to variations of the order parameter Ψ, leads to the Ginzburg-Landau equation:

$$\alpha\Psi + \beta|\Psi|^2\Psi + \frac{1}{2m}(-i\hbar\nabla - 2\mathrm{e}\mathbf{A})^2\Psi = 0\,. \tag{6}$$

For this problem, now in connection with the magnetic field, Maxwell equations have to be fulfilled:

$$\boldsymbol{\nabla} \times \boldsymbol{H} = \mathbf{J}\,. \tag{7}$$

With boundary conditions that $\Psi = 0$ at the surface of the superconductor and that in the most interior part we have Ψ_{max} constant in the absence of a magnetic field that can interfere with the superconducting effects (Simplified case with $\mathbf{A} = 0$), we arrive at $\alpha\Psi_{max} + \beta|\Psi_{max}|^2\Psi_{max} = 0$, with a trivial solution of $\Psi_{max} = 0$, which corresponds to the normal state of the superconductor for temperatures $T > T_c$, and $n_{s,max} \equiv |\Psi_{max}|^2 = -\alpha/\beta = \alpha_0(T - T_c)/\beta$ for $T < T_c$.
Solving (6) for the one dimensional case leads to the coherence length ξ. The coherence length is a measure of the shortest distance over which superconductivity may be established. It is also a measure of the spatial variation of the density of superconducting electrons. A small coherence length ξ would mean that the density can change rapidly. One consequence of its existence is that the boundary between a normal and superconducting region cannot be sharp because the density of superconducting electrons can rise from zero

in the normal region to its density n_s only gradually over a distance equal to about the coherence length. An illustration of the coherence length ξ and the penetration depth λ for a type I superconductor can be seen in figure 3.
For a type II superconductor, the penetration depth is greater than the coherence length. The result is that it is thermodynamically favorable for the magnetic field to penetrate the specimen.

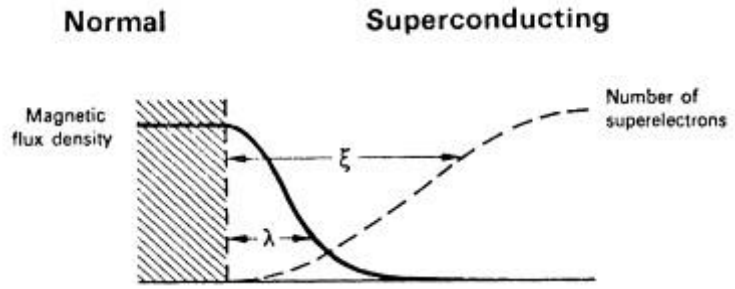

FIGURE 3: Schematic representation (taken from [7]) of the main superconducting parameters coherence length ξ and penetration depth λ for type I superconductors

The coherence length depends on the purity of the metal. If impurities are present, the coherence length is reduced. If there are so many impurities and defects that the mean free path σ in the normal conducting state becomes smaller than the BSC coherence length, then we have an effective coherence length:

$$\xi = \sqrt{\xi_0 \sigma}\,,$$

where ξ_0 is the coherence length in a perfectly pure superconductor, and ξ the actual measured coherence length in an impure metal or alloy.
Following from (2) by replacing n_s by $|\Psi|^2$ and taking into account that the change in Cooper-pairs is 2e, the penetration depth λ can also be expressed as:

$$\lambda(\mathrm{T}) = \sqrt{\frac{\mathrm{m}}{4\mu_0 \mathrm{e}^2 \psi_0^2}}\quad,$$

where ψ_0 is the equilibrium value of the order parameter deep inside the superconductor in the absence of an electromagnetic field.

2.5. Types of superconductors

As mentioned, superconductors can be divided into 2 classes according to how their superconducting state breaks down with an high enough applied magnetic field and can be classified by a single parameter, the Ginzburg-Laundau-parameter $\kappa = \lambda/\xi$. The H-T diagram for a bulk type I and II superconductor is presented in figure 4.

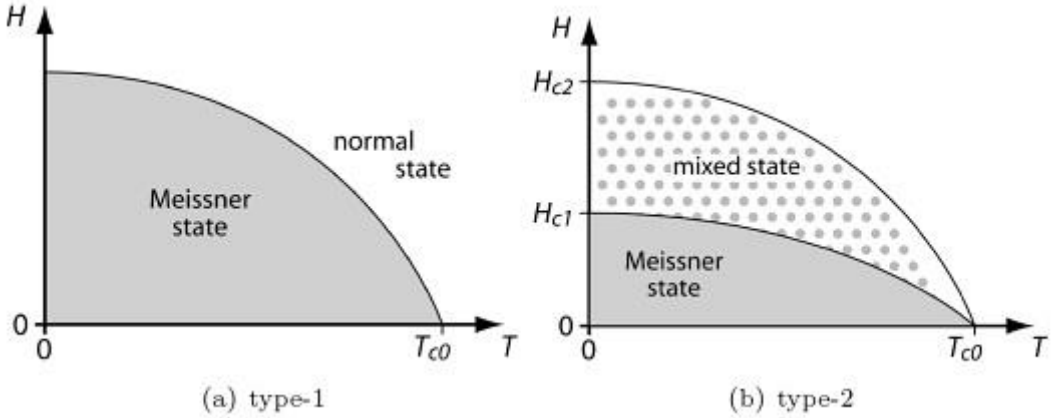

FIGURE 4: The H-T phase diagram of a single-gap (a) type I and (b) type II superconductor. (Taken from [9])

For $\kappa < 1/\sqrt{2}$, we have type I superconductors. In a type I superconductor, the applied magnetic field remains zero inside the superconductor until suddenly the superconductivity is destroyed when the strength of the applied field rises above a critical value H_c.
If $\kappa > 1/\sqrt{2}$, complete flux expulsion is no longer favorable and flux is allowed to penetrate the superconductor through cores known as vortices. This is a characteristic of type II superconductors.

Type II superconductors get into a mixed state once the applied magnetic field is raised past a critical value H_{c1} , in which an increasing amount of magnetic flux penetrates the material, but there remains a phase-coherence. This means that there exists a well defined phase-difference between the ends of a superconducting strip, for example. For small enough currents and sufficient "pinning" of the vortices, there is also zero resistance. At a second critical field H_{c2} , the superconductivity is destroyed.
Currents swirling around the normal cores generate magnetic fields parallel to the applied field. These tiny magnetic moments repel or attract each other and move to arrange themselves in an orderly array known as a fluxon lattice. This mixed phase helps to preserve superconductivity between H_{c1} to H_{c2}. It is very important that these vortices do not move in response to magnetic currents if superconductors are to carry large currents. Vortex movement results in resistivity. If a vortex moves fast through the strip, it will leave a normal conducting trail behind.
Another effect of current in superconducting strips is that wherever the vortex is, it feels a constant force that is pulling it to either side, depending on the current direction and its polarity.

Each vortex carries a fixed unit of magnetic flux $\phi_0 = h/2e$ and consists of a region of circulating supercurrent around a small normal conducting central core with radius ξ. The magnetic field is able to pass through the sample inside the vortex cores, and the circulating currents serve to screen out the magnetic field from the rest of the superconductor outside

the vortex. A schematic illustration of the distribution of the magnetic field and superconducting carriers near the vortex can be seen in figure 5.

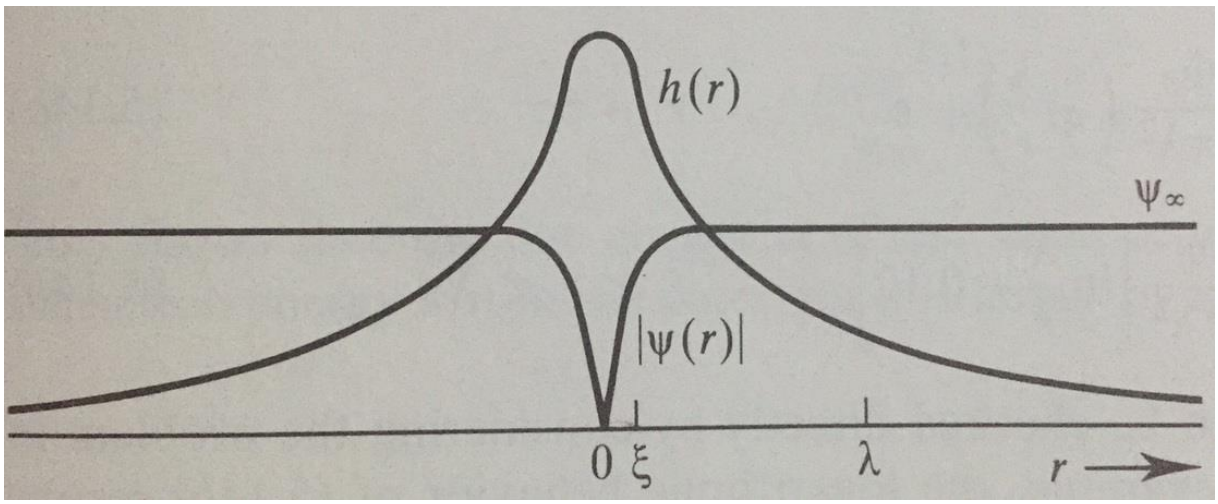

FIGURE 5: [2] Structure of an isolated Abrikosov vortex

3) Superconducting nanowire single-photon detectors (SNSPDs)

3.1. Basic Principle

Photon counts in a superconducting nanowire single-photon detector (SNSPD) are caused by the transition from a superconducting state with an applied current to the normal state. Even though the current detection models are not able to explain all experimental observations, there are a lot of indications that such a transition is triggered by vortices crossing the thin and narrow superconducting strip from one edge to another due to the Lorentz force [6].

According to [13], the typical SNSPD consists of a thin $(\sim 5\ nm)$ and narrow $(\sim 100\ nm)$ superconducting nanowire with the length typically of hundreds of micrometers, carrying a bias current *I* slightly below the critical current. The process is sketched in figure 6. The nanowire is maintained well below its critical temperature T_c (i). A photon is absorbed and results in a local disruption of the superconducting state that leads to a current redistribution(ii-iii). One way or another a complete cross-section becomes critical and switches into the normal state (iv-v), generating a measurable output voltage pulse across the strip on nanosecond time scales. One way this can happen is via the entry of a vortex and its movement across the strip. Measuring these voltage pulses, single photons can be detected and counted.
After the normal belt of the strip cools down, the strip returns to the superconducting state (vi).

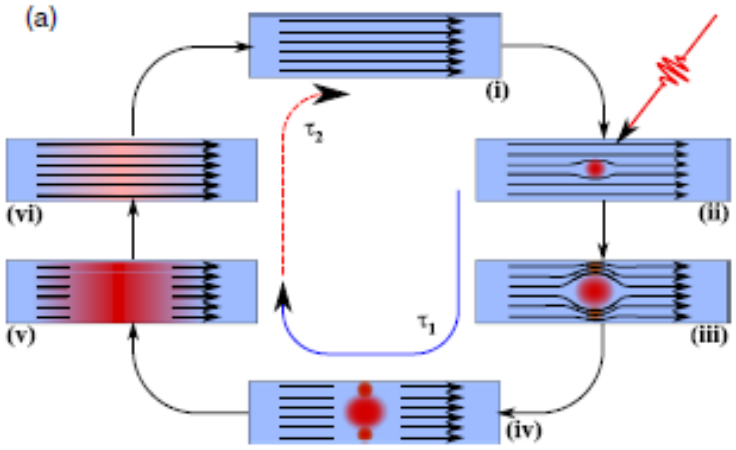

FIGURE 6: The basic principle of a superconducting nanowire single-photon detector (taken from [13])

Similar voltage pulses can be recorded in the absence of photons, called dark counts, and this introduces an uncertainty in the counting of single photons.
Vortex-assisted photon counts can happen here when the applied current decreases the potential energy barrier enough for a vortex to enter, and as a consequence of the Lorentz force acting on it, it crosses the belt releasing the energy $\phi_o I$ [3]. For currents $\gtrsim 0.6 I_c$, that is sufficient to create a normal belt across the entire width of the strip, extending to a few correlation lengths ξ along the strip. This process causes the transition from the

superconducting state of the strip to the normal state and induces a current redistribution accompanied by a measurable voltage pulse.
It was shown in [3] that in a thin d ($d \lesssim \xi \ll \lambda$) , and narrow ($w \ll \Lambda$) film the single-vortex crossing has the lowest energy barrier of various processes that all lead to a resistive cross-section. For this case ($d \lesssim \xi \ll \lambda$) we use the effective penetration depth $\Lambda = 2\lambda^2/d$ with London penetration depth λ and film thickness d.

3.2. Numerical detection model in SNSPD

The detection process in SNSPD may be divided into three steps: photon absorption, normal domain generation and electronic detection of the absorption event. The first and the last steps are well understood, but how the normal domain is generated is still not completely resolved. This thesis may add just a little bit towards how this domain may form by being able to simulate the influence of the magnetic field. In general, it is assumed that superconducting films are sufficiently thin so that the calculations can be restricted to two dimensions.
The origin of the coordinate system is in the centre of a rectangular strip, with the x-axis pointing along the length of the strip and in the direction of the current flow, and the y-axis in the transverse direction.

First, the photon is absorbed and the photon energy is converted into excitations of the superconductor. The assumption that [5] makes is that the whole photon energy is transferred to one single electron from the valence band. The excited electron is very energetic compared to the few meV of the superconducting gap. Quickly, it thermalizes, exciting many single electrons (by analogy to other excitations, even though they are real electrons, they are called quasiparticles) and phonons. Since all the phonons that are created are comparatively very energetic, the time-scales for them to find a new equilibrium at a higher temperature is much longer than the time it takes the quasiparticles to come to a quasi-equilibrium, so they are not considered at this stage.
Another assumption of [5] is that the electronic system is in thermal equilibrium, so one can directly relate the quasiparticle density n_{qp} to the cooper pair density n_{cp} at a certain position.

The number of superconducting electrons n_s is two times the number of cooper pairs n_{cp} , and normalized by the equilibrium situation n_s^0 where there is no quasiparticle yet and where thermally excited quasiparticles are neglected, we get:

$$\frac{n_s(\boldsymbol{r})}{n_s^0} = 1 - \frac{n_{qp}(\boldsymbol{r}.t)}{n_s^0}.$$

How that evolves is given by diffusion. In the first picoseconds, the excited electron will be locally created, and will scatter and diffuse according to:

$$\frac{\partial C_e(\boldsymbol{r},t)}{\partial t} = D_e \nabla^2 C_e(\boldsymbol{r},t)$$

with the probability density $C_e(\boldsymbol{r},t)$ to find it at a certain point at a certain time after the photon absorption.

And there, with a certain probability, it will create many new quasiparticles, more or less just above the superconducting gap. Once the quasiparticles are created, they will also diffuse, according to:

$$\frac{\partial C_{qp}(\boldsymbol{r},t)}{\partial t} = D_{qp}\nabla^2 C_{qp}(\boldsymbol{r},t) - \frac{C\_qp\ (\boldsymbol{r},t)}{\tau_r} + \frac{\zeta h\nu}{\Delta\tau_{qp}} e^{-\frac{t}{\tau_{qp}}} C_e(\boldsymbol{r},t)$$

with the first term being the diffusion term, then the quasiparticle annihilation term that describes the recombination of quasiparticles to form Cooper-pairs , and the creation term, where the first electron with energy $h\nu$ can still create quasiparticles with the efficiency ζ .
Having the distributions of superconducting electrons , it is possible to calculate the inhomogeneous current distribution and the potential energy for the vortex. This allows one to determine what current is necessary to reduce it to zero, so that a vortex can enter with 100% probability once a photon is absorbed, leaving a normal conducting electron trail behind and causing a voltage pulse. And for a vortex assisted photon count, that means 100% detection probability.
In this model, there are some limitations regarding the energy of the photon absorbed. The algorithm does not seem to work well for high energy photons that create fully normal conducting regions nor for situations when the current density approaches the depairing critical current density.

4) Applying a constant magnetic field

So far, external parameters bias current I_b and temperature *T* have been simulated in a 150 nm wide strip of different materials. Now, there is an important third external parameter that we are going to study: the magnetic field.
Like the bias current, an applied magnetic field B reduces the edge barrier and additionally breaks the symmetry between vortices and anti-vortices. Overall, it means an increase of photon count rates.
Here we simulated a strip of niobium nitride (NbN) superconductor, with an applied magnetic field perpendicular to it. The strip has a width of w $= 150\ nm$, thickness $d = 4\ nm$ and length $l = 1000\ nm$. Like in the previous model, the origin of the coordinate system is in the centre of a rectangular strip, with the x-axis pointing along the length of the strip and in the direction of the current flow, and the y-axis in the transverse direction.
The first thing to do was to calculate the microscopic value of the magnetic flux density h in the strip.
The inhomogeneous case, where a photon has been absorbed in the strip, cannot be solved analytically. The powerful software Matlab was used in this work to do all the numerical calculations. To simulate an infinitely long strip, in order to give us best result at the (0,y) positions that we want to measure, the 2 boundary conditions at the (-500,y) and (500,y) positions are Neumann boundary conditions , and the 2 boundary conditions at the (x,-75) and (x,75) positions are Dirichlet boundary conditions, setting the magnetic field to $h = 1$ at the edges. Since it is better for our purposes, this h is the applied magnetic field H normalized by $H_0 = \phi_0/2\mu_0 w^2$, with the vortex flux quantum ϕ_0 . So $h = H/H_0 = 1$ outside the strip.
The distribution of the field inside the strip can be calculated using the equation (1), with the difference that now, because of the photon absorption of a given energy, the penetration depth (2) will be position and time dependent:

$$\nabla^2 \mathrm{h}(\mathrm{x},\mathrm{y},\mathrm{t}) = \frac{\mathrm{h}(\mathrm{x},\mathrm{y},\mathrm{t})}{\lambda(\mathrm{x},\mathrm{y},\mathrm{t})^2} \ ,$$

$$\lambda(\mathrm{x},\mathrm{y},\mathrm{t})^2 = \frac{\mathrm{m}}{\mu_0 \mathrm{n_s}(\mathrm{x},\mathrm{y},\mathrm{t})\mathrm{e}^2}.$$

From the previous experiments from model [5], we have the position and time dependent areal density of superconducting electrons $n_{s,area}(x,y,t)$, for the homogeneous case before photon absorption (time=0) and for many other instants in time up to 50 ps after photon absorption, when we have an inhomogeneous distribution of superconducting electrons. Here we will need the volume density, so $n_s(x,y,t) = n_{s,area}(x,y,t)/d$.
Since all the length scales are in nanometers, it is convenient to also express the penetration depth in nanometers. So, converting from SI we get $\lambda(\mathrm{x},\mathrm{y},\mathrm{t})^2$ in nm^2:

$$\lambda(\mathrm{x},\mathrm{y},\mathrm{t})^2 = \frac{\mathrm{m}}{400\pi \mathrm{n_s}(\mathrm{x},\mathrm{y},\mathrm{t})\mathrm{e}^2}$$

To show that this numerical method of calculating h gives us the correct results, we compare it with the exact results for the homogeneous case (t=0) using equation (4).
As we can see in figure 7, there is almost perfect agreement between both methods.

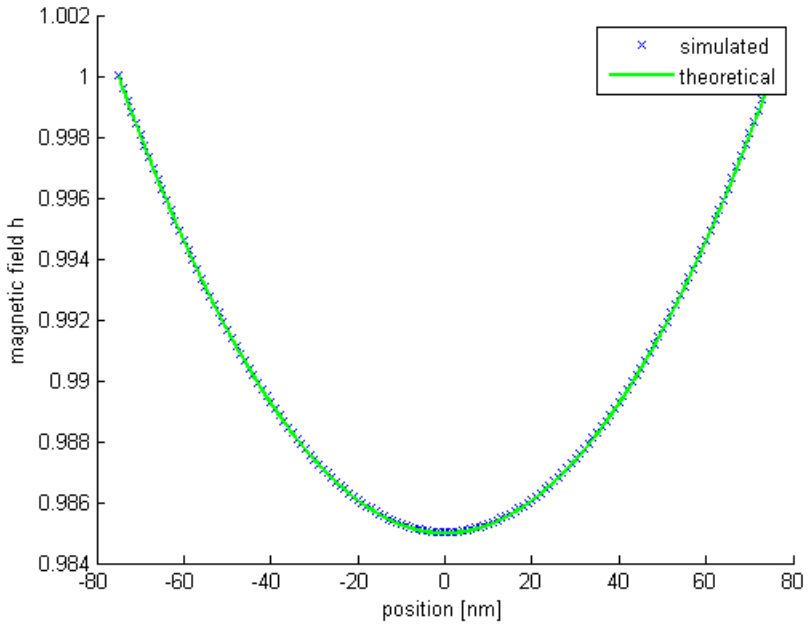

FIGURE 7: Perpendicular magnetic field h=1 for an infinitely long and thin homogeneous superconducting nanowire.

Next, we study the effect of the photon absorption on the penetration of the magnetic field inside the strip.

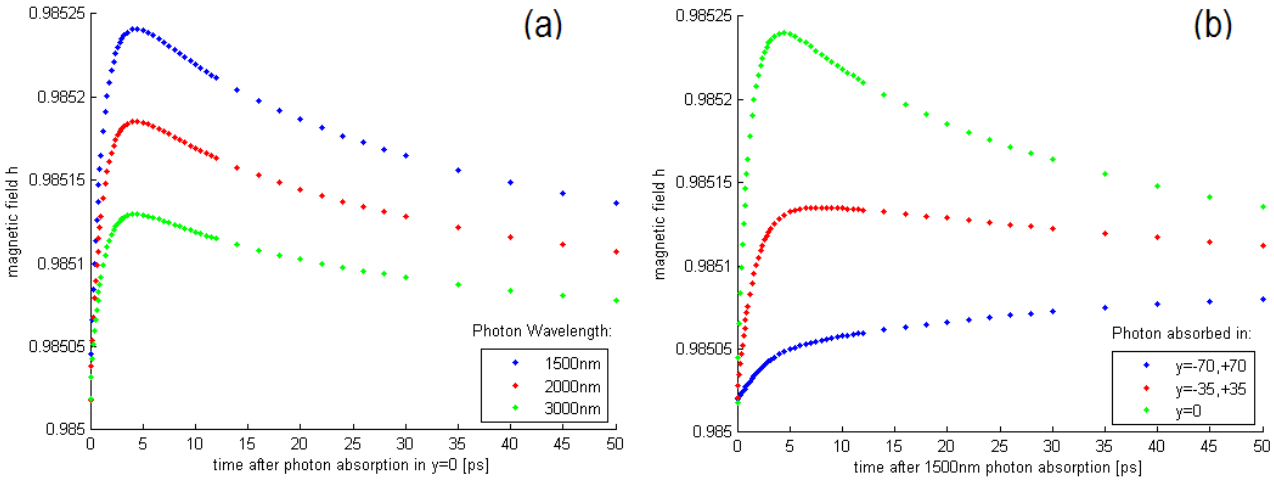

FIGURE 8: Variation of the minimum magnetic field h in the middle of the strip, as a function of the (a) time after photon absorption at position y=0 and different wavelengths, and (b) time after 1500 nm photon absorption at different positions.

In Figure 8 we clearly see that when a photon that has been absorbed is more energetic, it creates more quasiparticles in the middle of the strip, allowing the external magnetic field to penetrate more. As the time passes, the quasiparticles diffuse, and tend to recombine into cooper pairs, returning to the homogeneous state.
In figure 8 (b), the magnetic field in the middle of the strip was plotted. Therefore, the effect is strongest, when the photon is also absorbed in the center. When the photon is absorbed at the edge the quasiparticles have to diffuse towards the center and the opposite edge.
Knowing the field distribution and using equation (7), we can calculate the current distribution coming from the applied magnetic field (Meissner current):

$$\left(\nabla \times \mathrm{h}(\mathrm{x},\mathrm{y},\mathrm{t})\right) = \mathrm{j}(\mathrm{x},\mathrm{y},\mathrm{t}).$$

And since we are interested in the sheet current density, we have to multiply j with the thickness d,

$$\mathrm{j_s}(\mathrm{x},\mathrm{y},\mathrm{t}) = \mathrm{j}(\mathrm{x},\mathrm{y},\mathrm{t})\mathrm{d}\,.$$

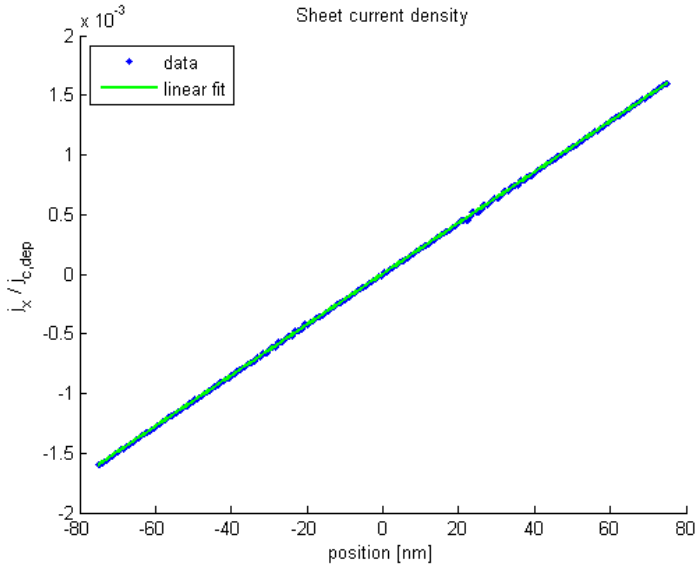

FIGURE 9: Sheet current density before photon absorption (homogeneous case).

To get to the next step now, we need to determine what influence does the magnetic field have on the vortices entering or not. For that, we need to calculate the vortex potential energy. The Gibbs free energy or vortex potential energy is made of 3 contributions: the vortex self energy and the energy from the bias current, both already calculated, and the new energy resulting from the screening currents. Now basically the question here is: what influence does the magnetic field have on this vortex potential and in particular on the maximum (entry barrier for the vortex)? To calculate the vortex potential energy from the current distributions calculated so far, we need the force density, that can be expressed as [2]:

$$\mathrm{f}(0,\mathrm{y},\mathrm{t}) = \mathrm{j_{s,x}}(0,\mathrm{y},\mathrm{t})\phi_0\,.$$

This gives the force, and the potential energy we calculate as the integral over the point of entry (0,75) to the position of a test vortex (0,y). Since ϕ_0 is constant, we obtain the result by simply integrating the current between the edge and the position of the test vortex. After that, to get the total potential energy, this just has to be added to the previously calculated results (vortex self energy and the energy from the bias current).
In order to be compatible with the results format from the previous experiments from model [5], one still needs to multiply the results with $\mathrm{H}_0/\varepsilon_0$, where $\varepsilon_0 = \phi_0^2 d/4\pi\mu_0\lambda^2$ is the characteristic vortex energy in a thin film.
The plots of the total vortex and anti-vortex potential energies can be seen in figures 10 and 11. They are very consistent compared to the analytical results in [3].

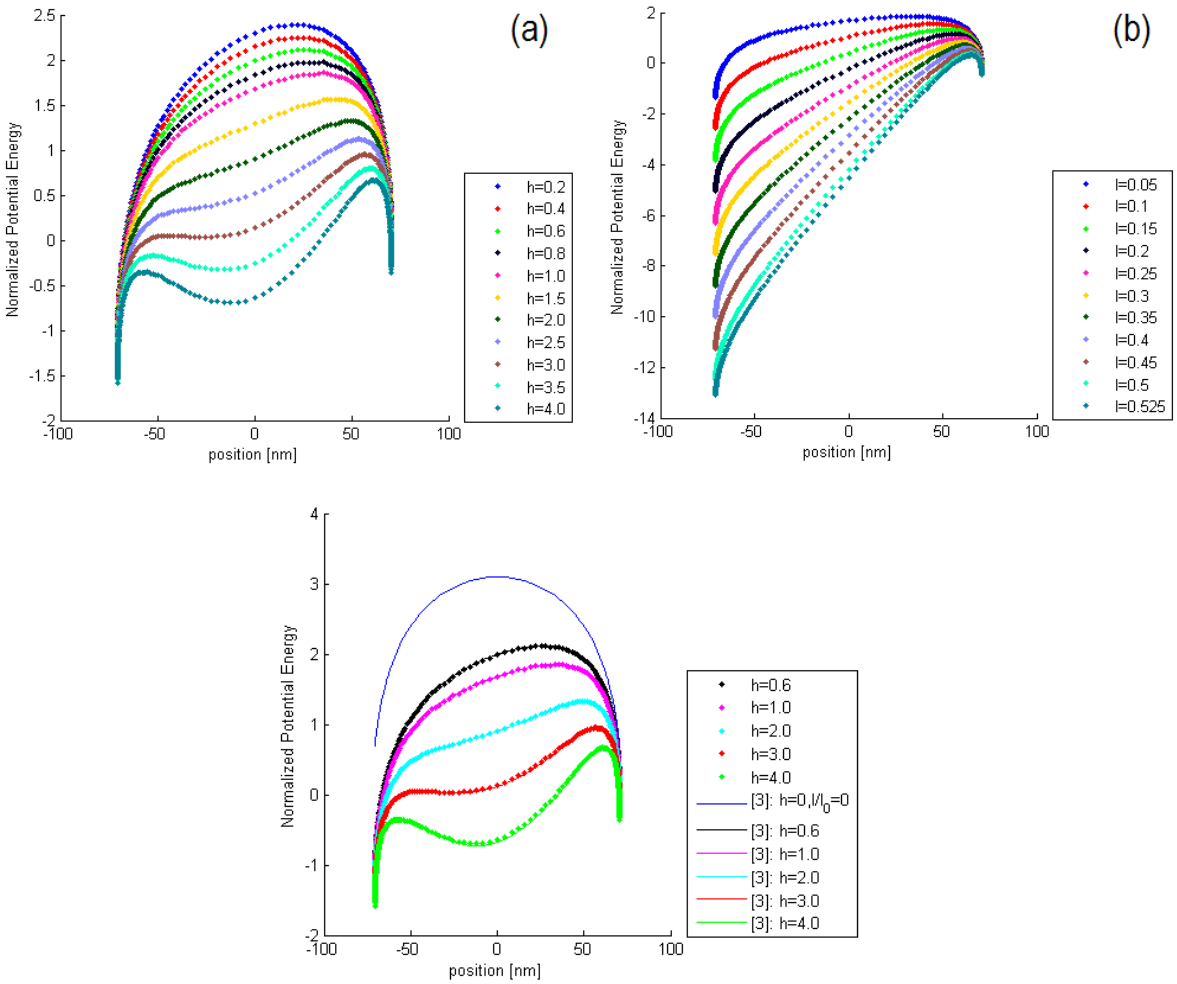

FIGURE 10: vortex potential energy in the homogeneous case (no photon absorbed yet), with (a) normalized bias current I=0.05 and varying applied magnetic field h and (b) applied magnetic field h=1 and varying normalized bias current I. In (c), we have the lines as plots from the analytical functions of [3], and we can see that our model matches almost perfectly. The line for h=0 and I/I_0=0 is the line of the vortex free energy, according to [3].

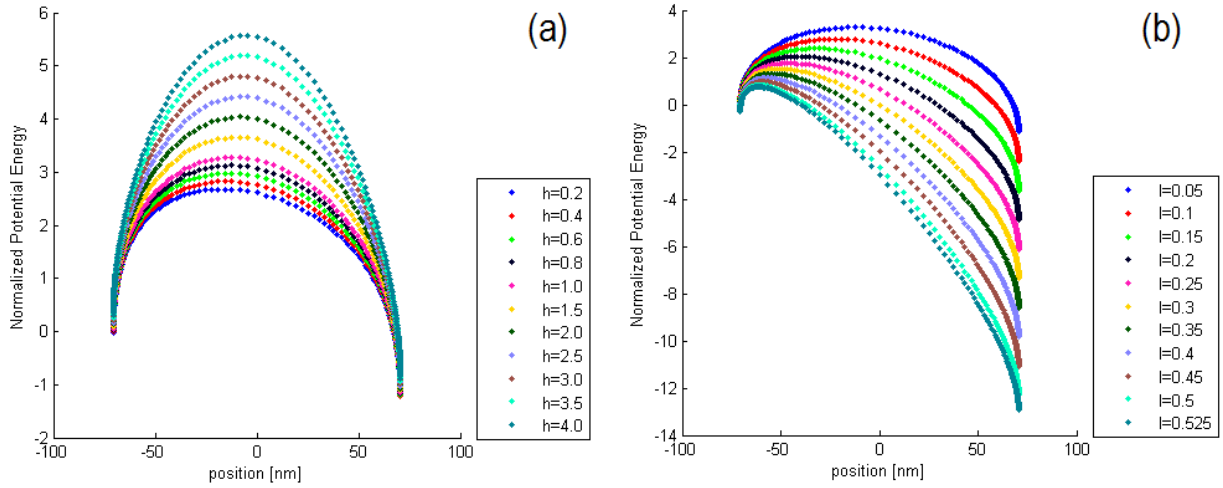

FIGURE 11: Anti-vortex potential energy in the homogeneous case (no photon absorbed yet), with (a) normalized bias current I=0.05 and varying applied magnetic field h and (b) applied magnetic field h=1 and varying normalized bias current I.

The results agree very well with [3] and [10], as we can see in figure 10 (c).This is the potential energy barrier that a vortex comming from the right would have to overcome in order to enter the superconducting strip.
An anti-vortex would enter from the left and would have to overcome this potential energy barrier. As we can see, for the case of the anti-vortex, an increasing magnetic field would increase the potential barrier.

5) Vortex-entry barrier and threshold current

For the simulations with magnetic field, the results of the experiments from model [5] for photons with wavelengths of 1000, 1300, 1400, 1500, 1600, 2000 and 3000 nm and various different bias currents at many different times are used, and the contributions of the magnetic fields $H/H_0 = 0.2, 0.4, 0.6, 0.8, 1.0, 1.5, 2.0, 2.5, 3.0, 3.5, 4.0$ for the potential energy are added to it. For every magnetic field applied, the threshold current is determined, that is, the lowest current necessary to reduce the edge barrier to zero.

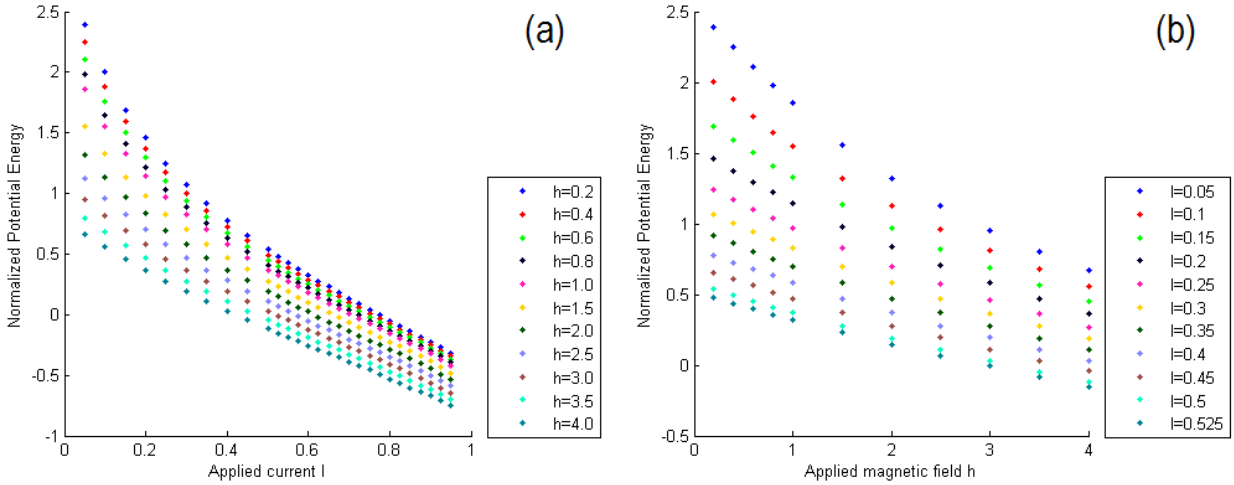

FIGURE 12: Barrier height for vortex entry for the homogeneous case, as a function of (a) applied current I for a given applied magnetic field h and (b) applied magnetic field h for a given applied current I.

From the plots in figure 12 we see that in the homogeneous case, where no photon has been absorbed yet, the energy barrier for a vortex to enter decreases with increasing applied current and magnetic field. As soon as this barrier becomes less than zero, vortices are expected to enter at a very high rate all along the strip, and that will lead ultimately to the destruction of the superconductivity. These points determine the experimental critical current.

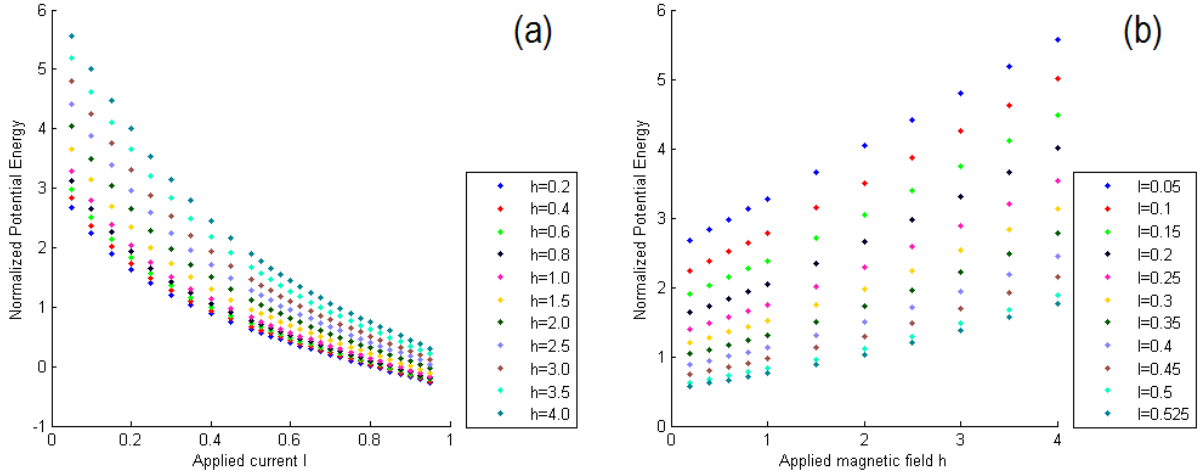

FIGURE 13: Barrier height for anti-vortex entry for the homogeneous case, as a function of (a) applied current I for a given applied magnetic field h and (b) applied magnetic field h for a given applied current I.

For the anti-vortex, we have that decreasing the magnetic field and increasing the applied current decreases the energy barrier.
Exactly where the results are not reliable anymore depends on the photon energy, that is, how many quasiparticles are produced and how much the superconducting electron density is reduced.
The more the potential energy is reduced, already at lower currents there will be situations where the velocity of the cooper pairs gets very close to the critical velocity at some part of the strip. So there will be strong non-linear effects and some parts may become normal conducting.
As the current is increased, these superconducting electrons cannot carry more current. The way that the quasiparticle distribution is calculated in [5] cannot adequately handle this situation, and the level of systematic errors increases.
For sufficiently low photon energies, things are handled very well, and we can determine the current where the potential is dropping below zero, that is, the threshold current for photon detection, with which there is a 100% probability of photon detection.
Now we look at what happens when we do have photon absorption. No analytical formula exists for the non-homogeneous case. Here we have to use our numerical approach.

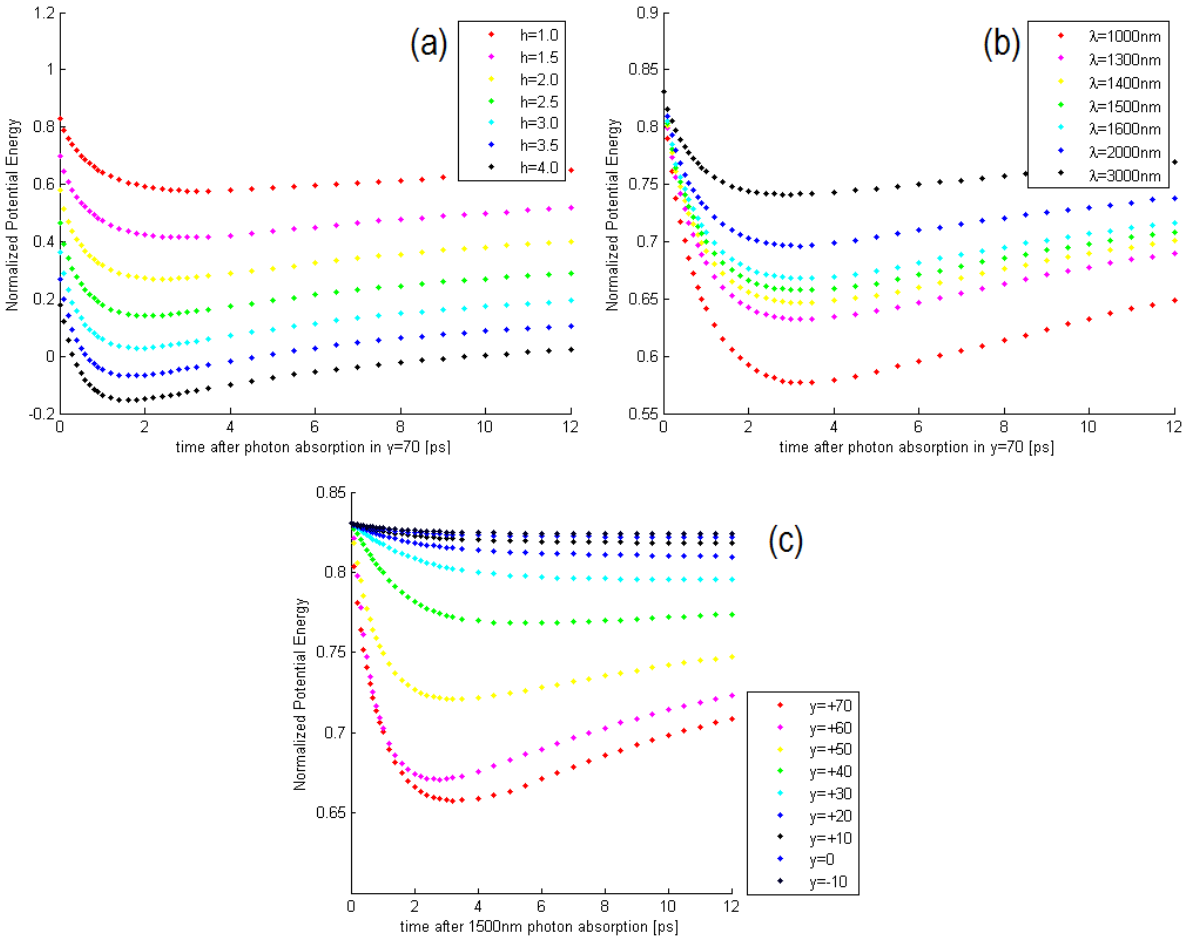

FIGURE 14: Barrier height for vortex entry for: (a) I=0.3 and a 1000 nm photon absorbed at position y=70 nm, as a function of time and applied magnetic field; (b) h=1, I=0.3 and a photon absorbed at position y=70 nm, as a function of time and photon wavelength; (c) h=1, I=0.3 and a 1500 nm photon absorption, as a function of time and absorption position.

In figure 14, we see the non-homogeneous case, where a photon of a given energy has been absorbed somewhere in the strip. Clearly, photons absorbed near the edge have much more

effect on decreasing the potential energy barrier. The maximal decrease of potential barrier is reached with a high energy photon absorbed near the edge that the vortex enters, in our case the positive edge. Increasing applied magnetic field or current lowers the barrier even more. For an anti-vortex, the maximal decrease of potential barrier is reached with a high energy photon being absorbed near the negative edge, decreasing applied magnetic field and increasing applied current.
Because for an anti-vortex we have a higher potential barrier for a positive applied magnetic field, leads to a higher threshold current for the anti-vortex potential energy to drop below zero.
But if for one photon absorption position the threshold current for an anti-vortex to enter is smaller than the threshold current for a vortex to enter, we would have two domains, one where the vortex is most likely to enter, and on the other the anti-vortex.
In figure 15 it is easy to see that the closer to the edge a photon is absorbed, the smaller is the current we have to apply for a vortex to enter, and consequently, to reach the highest photon detection efficiency.

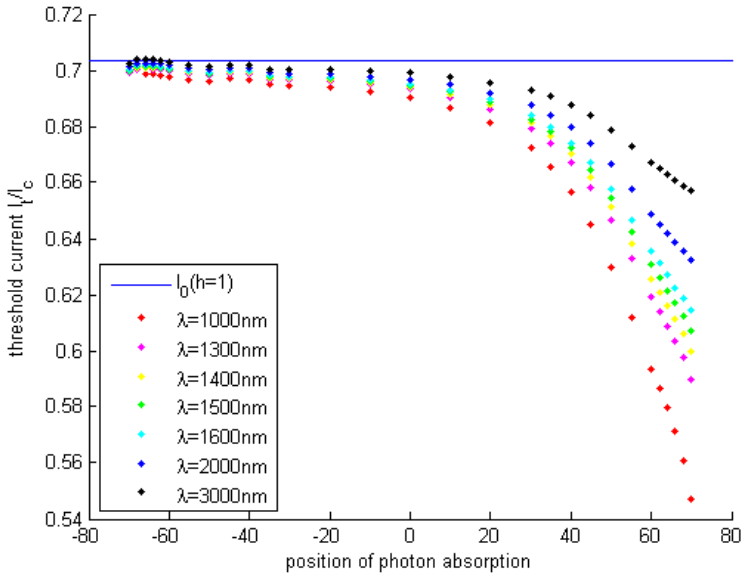

FIGURE 15: Scaled threshold current I_t/I_c , where I_c is the depairing critical current , for applied magnetic field h=1, as a function of position of photon absorption and photon wavelength. I_0 here is the current at which for that magnetic field of h=1, even without photon absorption, there will be vortices coming in (critical current of the strip for h=1).

One observation is that the smaller the photon energy is, the further up the curve is shifted, and the bigger is the applied current needed to detect it.
Another observation is that the curve seems to go down a lot near the edge compared to the center, therefore making the edges more sensitive to the detection of a photon than the center. This could be because in the center there is zero current from the magnetic field screening, and near the edges the current is strongest.
Plotting the threshold current for one given H/H_0 as a function of photon energy for every photon absorption position gives us a very good linear relation for every position, as we can see in figure 16. Fitting a line through every set of points for one position, we see that all the interception terms seem to converge at one point. Taking an average gives us the point I_0 , that is, the current as a function of H/H_0 where a vortex can enter even without photon absorption. The field dependent I_0 can be seen in figure 17.

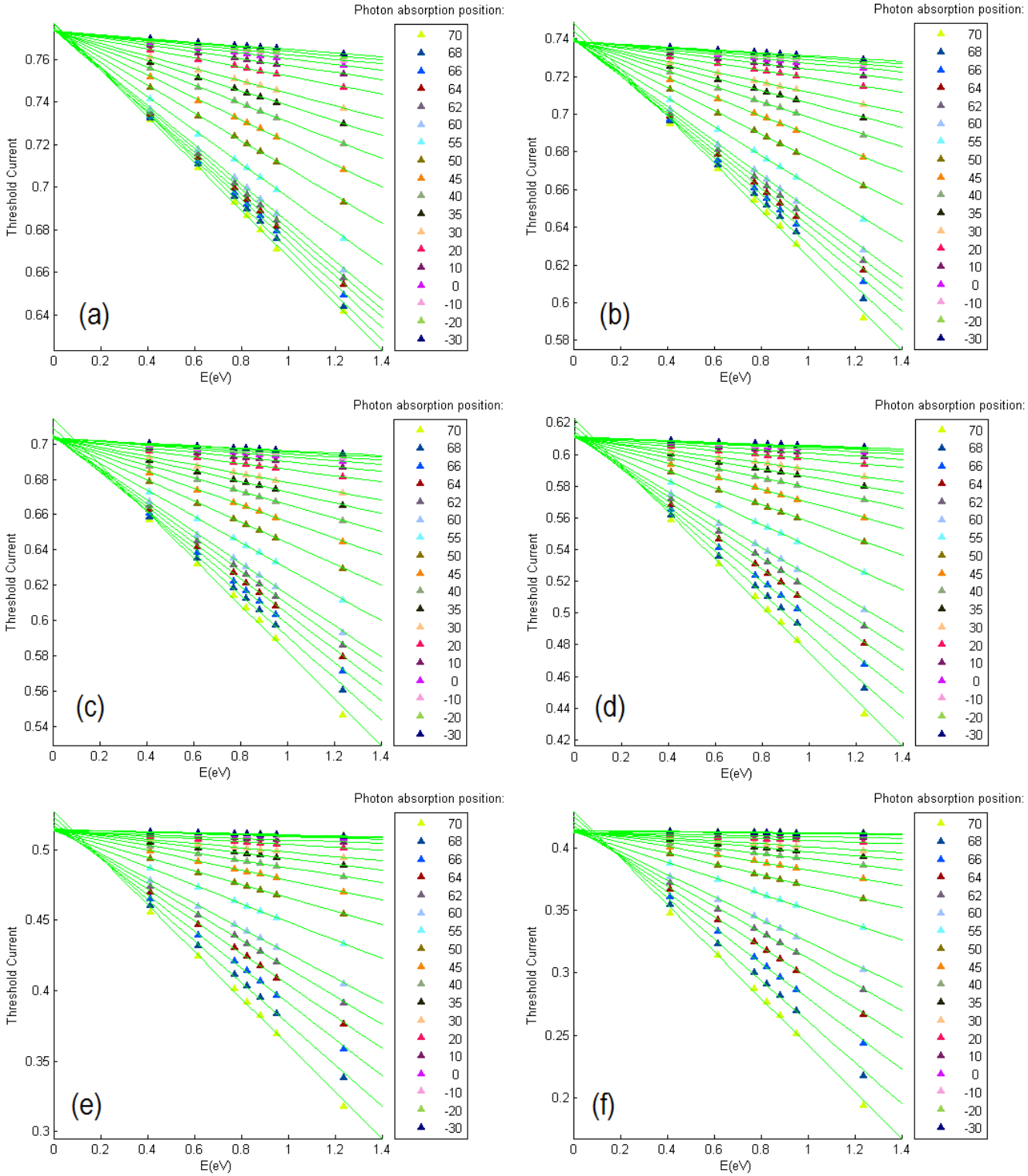

FIGURE 16: Plot of the threshold current as a function of photon energy and photon absorption position for (a) h=0.2, (b) h=0.6, (c) h=1, (d) h=2, (e) h=3 and (f) h=4. For clarity, only photon absorption positions up to y=-30 nm are plotted. The absorption positions are in nanometers and denote the difference to the center.

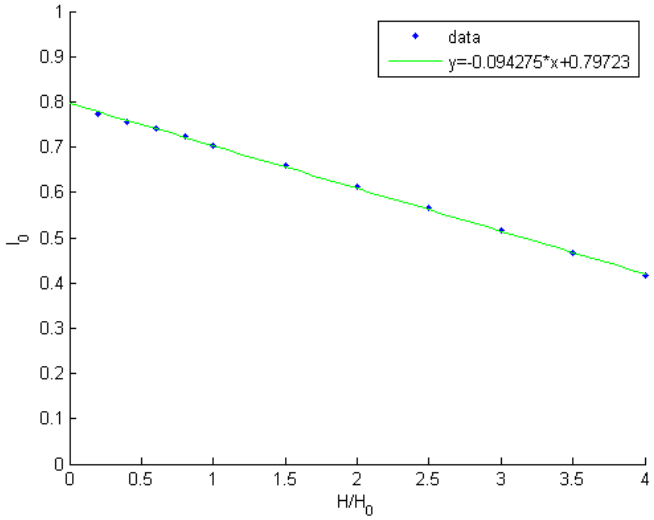

FIGURE 17: field dependent current I_0, as a function of H/H_0 where a vortex can enter even without photon absorption.

So now, we have a field dependent $I_0(H)$. The points seem to be in a very good linear relation also, so fitting a line through them gives the I_0 for which a vortex can enter without photon absorption and without an applied magnetic field, and that is: $I_0 = 0.79722$. And it gives also the magnetic field for which a vortex can enter without photon absorption and without a bias current, and that is: $/H_0 = 8.51258$. This agrees very well with [3] and [10]. Plotting the slopes as a function of H/H_0 for every position gives us figure 18. The relation again appears to be linear, so I fitted a line for each photon absorption position, and also plotted them to make it easier to read the graph.

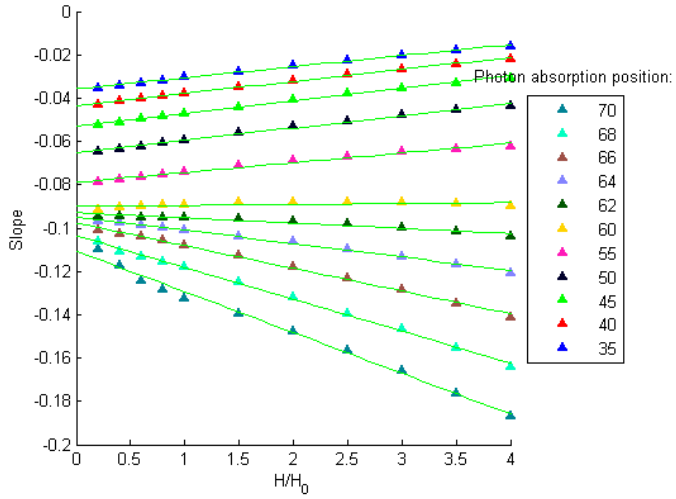

FIGURE 18: Slope of the linear relation between the threshold current and photon energy (as seen in figure 16), as a function of the applied magnetic field and photon absorption position.

Most important to understand here is that there are two competing effects that lead to a change in the potential barrier:

1. The reduction of n_S results in an effectively larger penetration depth, thus a lower screening current density. This leads to an increase of the barrier for vortex entry.

2. We have a redistribution of screening current and bias current caused by the non-homogeneous reduction of n_S, with the strongest increase near the absorption position (where and by how much exactly depends critically on the quasiparticle distribution). This leads to a decrease of the barrier for vortex entry.

These two effects together mean that when the absorption happens relatively close to the edge, the current flowing in the narrow region between the absorption point and the edge is squeezed, leading to a relatively large increase of the current density.
As we move away from the edges, this effect becomes increasingly less pronounced. But the overall reduction of the screening current is still there, and eventually, appears to be the dominant effect.
This can be seen in figure 18. The closer to the edge a photon is absorbed, the steeper the slope becomes, so the stronger the threshold current will decrease as a function of applied magnetic field and photon energy.
At position around 60, there seems to be no change in the slope for increasing applied magnetic field. This means, the two competing effects discussed are in equilibrium.
At position 55 the linear relation changes sign, meaning that the threshold current would decrease for increasing photon energy and applied magnetic field.

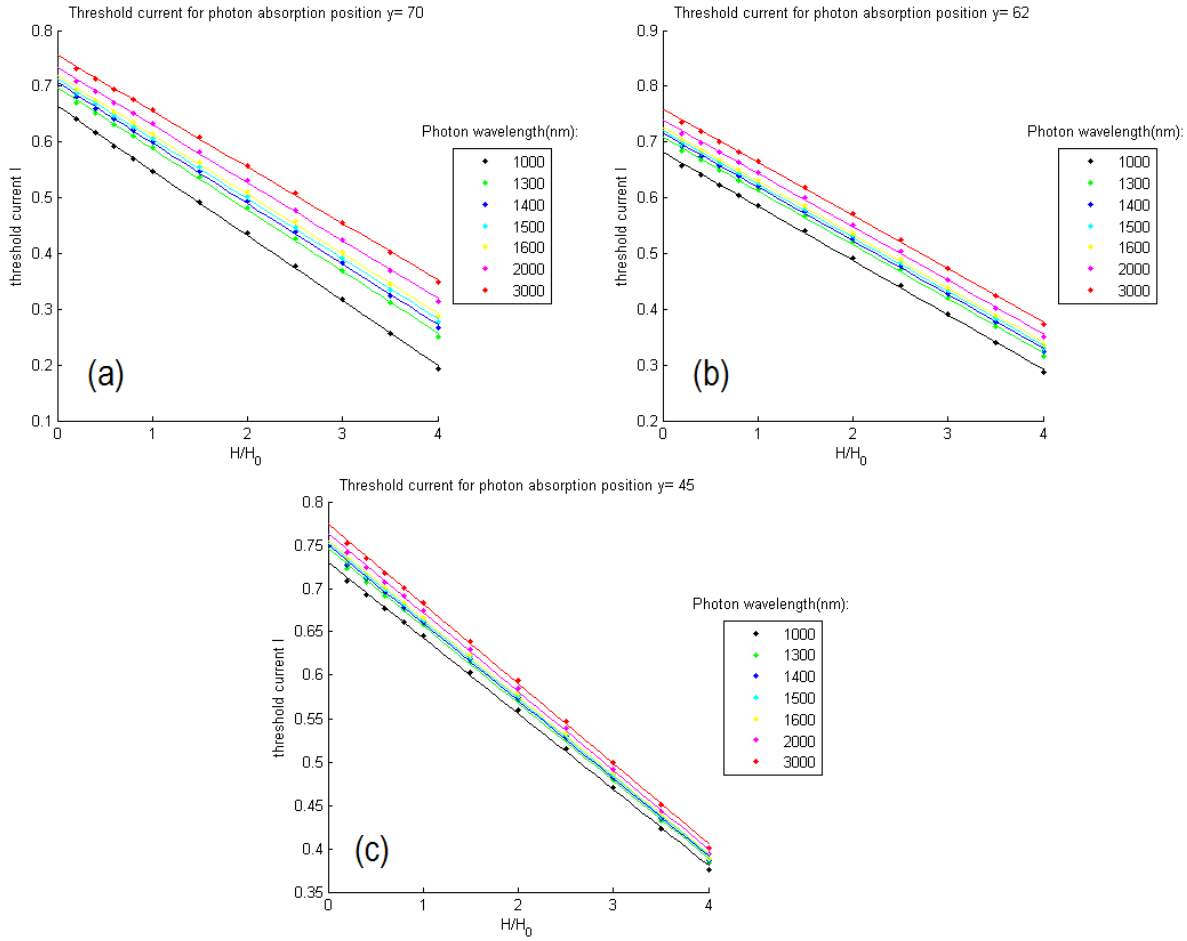

FIGURE 19: Threshold current as a function of applied magnetic field and photon wavelength, for a photon absorbed in (a) y=70 nm, (b) y=62 nm and (c) y=45 nm.

One can also see that in figure 19 for fixed photon positions. Very close to the edge the lines diverge for increasing applied magnetic field. But at y=45, the lines seem to converge.

6) Conclusion

In this thesis we numerically simulated the effect of various applied magnetic fields on the vortex assisted photon count of SNSPDs, for the homogeneous case, where no photon has been absorbed, and for the non-homogeneous case, where we have photons absorbed at various y positions across a 150 nm wide detector.
As expected, an applied magnetic field reduces the potential barrier for a vortex to enter, leading to a detection event. We found out that the effect of the magnetic field also depends on the photon absorption position. We have a much greater influence of the magnetic field for photons absorbed near the edge of the detector strip, because of the current crowding effect around the position of maximum quasiparticles concentration created by the photon absorbed.
This effect hasn't been experimentally observed so far, but it could possibly be measured directly. There have been already measurements of the magnetic field effects for these detectors, but without the resolution of where particular photons have been absorbed.
In [18] they perform a numerical study of an idea of how to measure this position dependence, and in [19] they measured it successfully, using different light polarizations. It was done without the magnetic field. But it could be redone, in principal, with an applied magnetic field.
The next step would be trying to relate these results to experimental measurements that have been done already.

7) References

[1] C. Kittel. *Einführung in die Festkörperphysik*. Oldenbourg, 2006.
[2] M. Tinkham. *Introduction to superconductivity*. McGraw-Hill, Inc., 1996.
[3] L. N. Bulaevskii, Matthias Graf, and V. G. Kogan , Vortex-assisted photon counts and their magnetic field dependence in single-photon superconducting detectors , *Phys. Rev. B,* vol 85 , 014505, 2012.
[4] 1L. N. Bulaevskii, M. J. Graf, C. D. Batista, and V. G. Kogan, *Phys. Rev. B,* vol 83, 144526, 2011.
[5] A. Engel and A. Schilling, "Numerical analysis of detection-mechanism models of superconducting nanowire single-photon detectors"*, J. Appl. Phys.*, vol 114, 214501, 2013.
[6] A. Engel, J J Renema, K Il'in, A Semenov, "Detection mechanism of superconducting nanowire single-photon detectors", *Supercond. Sci. Technol*., vol 28, 114003, 2015.
[7] A.C. Rose-Innes and E.H. Rhoderick, *Introduction to Superconductivity*, Pergamon Press plc, 1978.
[8] Charles P. Poole JR, Ruslan Prozorov, Horacio A. Farach, Richard J. Creswick, *Superconductivity*, Elsevier Inc, 2014.
[9] Victor V Moshchalkov, Joachim Fritzsche , *Nanostructured Superconductors*, World Scientific Publishing Co. Pte. Ltd., 2011.
[10] John R. Clem, Yasunori Mawatari, G.R.Berdiyorov and F.M.Peeters, Predicted field-dependent increase of critical currents in asymmetric superconducting nanocircuits*, Physical Review B,* vol 85, 144511, 2012.
[11] E.A.Dauler, M.E.Grein, A.J. Kerman, F.Marsili, S. Miki, S.W.Nam, M.D.Shaw, H. Terai, V.B. Verma , T. Yamashita, "Review of superconducting nanowire single-photon detector system design options and demonstrated performance, *Opt. Eng*, vol 53, 081907, 2014.
[12] R.H. Hadfield, "Single-photon detectors for optical quantum information applications", *Nature Photonics*, vol 3, 669-740, 2009.
[13] C.M. Natarajan, M.G. Tanner, R.H.Hadfield, "superconducting nanowire single-photon detectors: physics and applications, *Superconductor Science and Technology*, vol 25, 063001, 2012.
[14] A. Engel, A. Schilling, K Il'in, M. Siegel, *Phys. Rev. B*, vol 86, 140506, 2012.
[15] R. Lusche, A. Semenov, Y. Korneeva, A. Trifonov, A. Korneev, G. Gol'tsman and H.-W. Hubers, *Phys. Rev. B*, vol 89, 104513, 2014.
[16] J.J. Renema et al., *Appl. Phys. Lett*., vol 106, 092602, 2015.
[17] D. Yu. Vodolazov, Yu. P. Korneeva, A. V. Semenov, A. A. Korneev and G. N. Goltsman, *Phys. Rev. B*, vol 92, 104503, 2015.
[18] Q. Wang, J.J. Renema, A. Engel, M.P. van Exter and M.J.A. de Dood, *Optics Express*, vol 23, 24873-24887, 2015.
[19] J.J. Renema et al., *Nano Letters*, vol 15, 4541-4545, 2015.

8) Acknowledgement

I would like to thank my supervisor Dr. Andreas Engel, for all the excellent explanations and superb guidance throughout my work. Furthermore, I would like to thank Prof. Dr. A. Schilling for giving me the opportunity to do such an interesting bachelor work at his research group.